1101 Market Street, Chattanooga, Tennessee 37402

CNL-20-061

August 27, 2020

10 CFR 50.90

ATTN: Document Control Desk
U.S. Nuclear Regulatory Commission
Washington, D.C. 20555-0001

Watts Bar Nuclear Plant, Units 1 and 2
Facility Operating License Nos. NFP-90 and NFP-96
NRC Docket Nos. 50-390 and 50-391

Subject: **Response to NRC Request for Additional Information Regarding Application to Implement the FULL SPECTRUM™[1] LOCA (FSLOCA™[1]) Methodology for Loss-of-Coolant Accident (LOCA) Analysis and New LOCA-specific Tritium Producing Burnable Absorber Rod Stress Analysis Methodology (WBN-TS-19-04) (EPID L-2020-LLA-0005)**

References:
1. TVA Letter to NRC, CNL-19-051, "Application to Implement the FULL SPECTRUM™[1] LOCA (FSLOCA™[1]) Methodology for Loss-of-Coolant Accident (LOCA) Analysis and New LOCA-specific Tritium Producing Burnable Absorber Rod Stress Analysis Methodology (WBN TS 19-04)," dated January 17, 2020 (ML20017A338)

2. NRC Electronic Mail to TVA, "Watts Bar Nuclear Plant, Units 1 and 2 - Request for Additional Information Regarding Request to Implement the FULL SPECTRUM™ LOCA Methodology (EPID L-2020-LLA-0005)," dated July 14, 2020 (ML20196L862)

In Reference 1, Tennessee Valley Authority (TVA) submitted a request for amendments to Facility Operating License (OL) Nos. NFP-90 and NFP-96 for the Watts Bar Nuclear Plant (WBN) Units 1 and 2, respectively. This license amendment request (LAR) revises the WBN Units 1 and 2 Technical Specification (TS) 5.9.5, "Core Operating Limits Report," to replace the loss-of-coolant accident (LOCA) analysis evaluation model references with reference to the FULL SPECTRUM™ Loss-of-Coolant Accident (FSLOCA™) Evaluation Model analysis

[1] FULL SPECTRUM and FSLOCA are trademarks of Westinghouse Electric Company LLC

applicable to WBN Units 1 and 2, with replacement steam generators. The proposed change also revises the WBN Unit 2 Operating License (OL) condition 2.C(4) to reflect the implementation of the FSLOCA Evaluation Model methodology. The proposed change also revises WBN Unit 1 TS 4.2.1, "Fuel Assemblies," to delete discussion of Zircalloy fuel rods.

In Reference 2, the Nuclear Regulatory Commission (NRC) provided a request for additional information (RAI) and requested a response by August 27, 2020. Enclosure 1 to this letter provides the response to the RAI.

Enclosure 1 contains information that Westinghouse Electric Company LLC (Westinghouse) considers to be proprietary in nature, based on information provided by Westinghouse to TVA in report WAT-D-12626-P, Revision 1, and from Pacific Northwest National Laboratory in report TTP-20-105, pursuant to 10 CFR 2.390, "Public inspections, exemptions, requests for withholding," paragraph (a)(4). Enclosure 2 contains a non-proprietary version of Enclosure 1. Enclosure 3 provides the Westinghouse Application for Withholding Proprietary Information from Public Disclosure CAW-20-5080 affidavit supporting this proprietary withholding requests. The affidavit sets forth the basis on which the information may be withheld from public disclosure by the NRC and addresses with specificity the considerations listed in paragraph (b)(4) of Section 2.390. Accordingly, TVA requests that the information which is proprietary to Westinghouse be withheld from public disclosure in accordance with 10 CFR Section 2.390. Correspondence with respect to the copyright or proprietary aspects of the items listed above or the supporting Westinghouse affidavit should reference CAW-20-5080 and should be addressed to Camille T. Zozula, Manager, Regulatory Compliance & Corporate Licensing, Westinghouse Electric Company, 1000 Westinghouse Drive, Suite 165, Cranberry Township, Pennsylvania 16066.

This letter does not change the no significant hazard considerations nor the environmental considerations contained in Reference 1. Additionally, in accordance with 10 CFR 50.91(b)(1), TVA is sending a copy of this letter and the enclosure to the Tennessee Department of Environment and Conservation.

There are no new regulatory commitments associated with this submittal. Please address any questions regarding this submittal to Gordon Williams, Senior Manager (Acting), Fleet Licensing, at (423) 751-2687.

I declare under penalty of perjury that the foregoing is true and correct. Executed on this 27th day of August 2020.

Respectfully,

James Barstow
Vice President, Nuclear Regulatory Affairs & Support Services

Enclosures:

1. Response to NRC Additional Request for Additional Information (Proprietary)
2. Response to NRC Additional Request for Additional Information (Non-Proprietary)
3. Westinghouse Electric Company LLC Application for Withholding Proprietary Information From Public Disclosure (Affidavit CAW-20-5080)

cc (Enclosures):

NRC Regional Administrator - Region II
NRC Resident Inspector – Watts Bar Nuclear Plant
NRC Project Manager – Watts Bar Nuclear Plant
Director, Division of Radiological Health - Tennessee State Department of Environment and Conservation

Response to NRC Additional Request for Additional Information (Non-Proprietary)

NRC Introduction

By application dated January 17, 2020 (Agencywide Documents Access and Management System (ADAMS) Accession No. ML20017A338), pursuant to Section 50.90 of Title 10 of the Code of Federal Regulations (10 CFR), Tennessee Valley Authority (TVA) submitted a license amendment request (LAR) for the Watts Bar Nuclear Plant, Units 1 and 2 (WBN). The proposed changes would: revise WBN Units 1 and 2 Technical Specification (TS) 5.9.5, "Core Operating Limits Report," to replace the loss-of-coolant accident (LOCA) analysis evaluation model references with reference to the FULL SPECTRUM™ Loss-of-Coolant Accident (FSLOCA™) Evaluation Model analysis applicable to WBN Units 1 and 2, with replacement steam generators; revise the WBN Unit 2 Operating License Condition 2.C(4) to reflect the implementation of the FSLOCA Evaluation Model methodology; and, revise WBN Unit 1 TS 4.2.1, "Fuel Assemblies," to delete discussion of Zircalloy fuel rods. TVA is also requesting approval of the new LOCA-specific Tritium Producing Burnable Absorber Rod (TPBAR) stress analysis methodology to evaluate the integrity of the TPBARs for conditions expected during a large break LOCA (LBLOCA).

The U.S. Nuclear Regulatory Commission (NRC) staff has been auditing several analyses documents that were not provided as part of the LAR. The documents listed below were made available to the NRC staff as part of its audit request (ADAMS Accession No. ML20120A021) via an online portal (i.e., CERTEC electronics library).

1. *WCAP-18429-P Revision 0, "Watts Bar Units 1 and 2 TPBAR Structural Integrity Analysis for the Large Break Loss of Coolant Accident (LBLOCA)," Westinghouse, March 2019.*
2. *TTP-1-3101 Revision 1, "Development of a Metric for Evaluation of TPBAR Structural Integrity During LBLOCA Event," Westinghouse/TVA/PNNL, April 2019*
3. *PNNL-TTP-1-3123, Revision 1, Tritium Technology Program "Stainless Steel Burst Stress Curve Evaluation," PNNL/TVA, March 2020.*
4. *PNNL TTP-3-714 Revision 0, "Thermal Creep Rupture Model Development for IOC Behavior of TPBARs," PNNL/TVA, March 2020.*
5. *PNNL TTP-3-721 Revision 1, "High Temperature Fracture Models for Assessment of TPBAR Cladding Survivability During LOCA," PNNL/TVA, April 2020.*
6. *Application to Implement the FULL SPECTRUM LOCA (FSLOCA) Methodology for Loss-of-Coolant Accident (LOCA) Analysis," and New LOCA-specific Tritium Producing Burnable Absorber Rod Stress Analysis Methodology (WBN-TS-19-04) (LAR)*

As a result of the NRC staff's audit of these documents and review of the LAR, the staff requests the following additional information.

SFNB D-RAI 1

Section 4.2.2 of Enclosure 1 of the LAR summarizes the LOCA-specific TPBAR cladding stress analysis methodology to determine the potential TPBAR cladding mechanical rupture under LBLOCA temperature and differential pressure conditions. The stress analysis of the TPBAR following an LBLOCA is performed assuming conditions as calculated using the

WCOBRA/TRAC-TF2 (WCT-TF2) code, the thermal-hydraulic code associated with the FSLOCA Evaluation Model.

(a) Provide details of reactor vessel, core, loop, emergency core cooling, and safety injection (SI) models used in the WCOBRA/TRAC-TF2 (WCT-TF2) code. The response should include the location of TPBARs with respect to location of fuel rods, hot assembly, guide tube, instrumentation tube, and burnable poison.

*(b) **[[** **]]**. Provide justification for this assumption.*

*(c) TVA states that the TPBAR figure-of-merit (for rapid burst failure mode and thermal creep rupture node) calculation is performed **[[** **]]**. Provide the rationale for this assumption.*

TVA Response to SFNB D-RAI 1(a)

Figure 1 provides a vertical view of the WBN Units 1 and 2 vessel (3D) noding. The elevations shown at the left are relative to the inside bottom of the reactor vessel. The values within the squares are the channel numbers, and the values within the circles with arrows attached to them are the horizontal flow gap numbers. A gap is used to define a lateral (transverse) flow path between channels located within a section. Positive flow is in the direction indicated by the arrow. WCOBRA/TRAC-TF2 assumes the existence of a vertical flow path between vertically stacked channels, unless specified otherwise by input. Upward axial flow is considered as positive flow.

Figure 1 illustrates that the reactor vessel is divided into ten vertical sections, and that several of the vessel sections are subdivided into two or more levels.

Core Model

The WCOBRA/TRAC-TF2 code allows for modeling of heated and unheated conductor geometries. Unheated conductors are used to model metal structures in the reactor vessel (e.g., lower core plate, reactor vessel wall, core barrel, upper core plate, guide tubes, support columns). These conductors are connected to the appropriate vessel channels. For heated conductors, the code allows for a detailed radial and axial noding, and for the nuclear rod, other fuel related inputs (e.g., rod internal pressure, pellet temperatures, fuel rod molar fractions, clad thickness, fuel theoretical density) can also be specified. There are **[**

]a,c

Loop Model

Figure 3 presents the WBN Units 1 and 2 WCOBRA/TRAC-TF2 loop (1D network) noding diagram, with a more detailed noding diagram for the steam generators in Figures 4 and 5. Component numbers and junctions are indicated by rectangular and circular boxes, respectively. The loop 1D hydraulic network consists of the major components in the primary system outside the reactor vessel (e.g., pipes, tees, pumps, valves, accumulators, the pressurizer, associated metal structures). As with the vessel model, each component in the one-dimensional loop can have various hydraulic cells to allow for changes in geometry to be modeled along the component. In the input structure, each component is identified by a module title, unique component number, and junctions that connect it to adjacent hydraulic components. The interface junctions existing between one-dimensional components and vessel channels are defined in the code input.

[

]a,c

Emergency Core Cooling and Safety Injection Model

The emergency core cooling system (ECCS) for WBN Units 1 and 2 consists of four accumulator tanks, two centrifugal charging pumps, two high head safety injection (HHSI) pumps, and two low head safety injection (LHSI) pumps. Each pump is connected to injection lines, which are headered with the accumulator injection lines, with the exception of the charging pumps, which are connected directly to the cold legs. [

]a,c The pumped safety injection flow is modeled assuming the loss of one train of safety injection pumps (one charging, one HHSI, and one LHSI). The loss of one train of safety injection is considered as the limiting single failure assumption.

The safety injection flow is calculated assuming the least resistive line spills to containment pressure for breaks larger than the accumulator line inner diameter (LBLOCA).

The safety injection is initiated when the low pressurizer pressure safety injection setpoint is reached. **[**

][a,c]

a,c

Figure 1: Watts Bar Units 1 and 2 Vessel Model Noding Diagram (Vertical View)

[a,c]

Figure 2: Assemblies Included in the Low Power Periphery

a,c

Figure 3: Watts Bar Units 1 and 2 WCOBRA/TRAC-TF2 Model Loop Layout

a,c

Figure 4: Watts Bar Units 1 and 2 WCOBRA/TRAC-TF2 Loops 1 and 2 Steam Generator Model Layout

a,c

Figure 5: Watts Bar Units 1 and 2 WCOBRA/TRAC-TF2 Loops 3 and 4 Steam Generator Model Layout

TVA Response to SFNB D-RAI 1(b) and (c)

The TPBAR cladding temperature is assumed to equal the adjacent fuel rod cladding temperature **[**

][a,c]

Section 2.15.5.1 of the Tritium Production Core (TPC) Topical Report (Reference 2, which was approved by the NRC in Reference 3) examined the response of the TPBAR to an LBLOCA considering the time-dependent effects of the various heat transfer mechanisms. As stated in Reference 2:

> *"The TPBAR generates minimal heat during a LOCA and is heated primarily by radiation from the fuel rods to the fuel assembly guide thimble and radiation from the thimble across the gap to the TPBAR. Convection of the steam and entrained liquid, on the outer thimble surface, provides cooling comparable to that experienced by the fuel rods."*

Simulations with a modified version of the LOCTA_JR fuel rod response code were performed with Appendix K LBLOCA boundary conditions, with results for the TPBAR as replicated in Figure 6 (Figure 2.15.5-1 of Reference 2). As described in Section 2.15.5.1 of Reference 2, LOCTA_JR uses the cladding temperature of the surrounding fuel rods and the core steam and entrained liquid convective heat transfer coefficients and temperatures as boundary conditions for the calculation of the TPBAR response within the fuel assembly guide thimble. Use of the LOCTA_JR code for TPBAR modeling in the TPC was approved by the NRC in Reference 4.

As shown in Figure 6, the fuel assembly thimble temperature leads the TPBAR cladding temperature with respect to time. In periods of heating, the thimble temperature heats sooner and faster than the TPBAR, and in periods of cooling, the thimble temperature cools sooner and faster. In the refill and late reflood phase of the transient (up to 200 seconds in Figure 6), when temperatures are increasing, the TPBAR cladding temperature will follow the thimble temperature and tend to remain lower until after the temperature peak is reached.

The TPBAR cladding temperature **[**

]a,c

References

1. WCAP-17642-P-A, Revision 1, “Westinghouse Performance Analysis and Design Model (PAD5),” dated November 2017
2. NDP-98-181, Revision 1, “Tritium Production Core (TPC) Topical Report,” dated February 1999
3. NUREG-1672, “Safety Evaluation Report related to the Department of Energy’s Topical Report on the Tritium Production Core,” dated May 1999
4. NRC letter to TVA, “Safety Evaluation of LOCTA_JR Code for Loss-of-Coolant Accident Analysis of Fuel Rods – Watts Bar Nuclear Plant, Unit 1, and Sequoyah Nuclear Plant, Units 1 and 2 (TAC Nos. MA9520, MA9583, MA9584),” dated January 17, 2001 (ML010170152)
5. WCAP-16996-P-A, Revision 1, “Realistic LOCA Evaluation Methodology Applied to the Full Spectrum of Break Sizes (FULL SPECTRUM LOCA Methodology),” dated November 2016

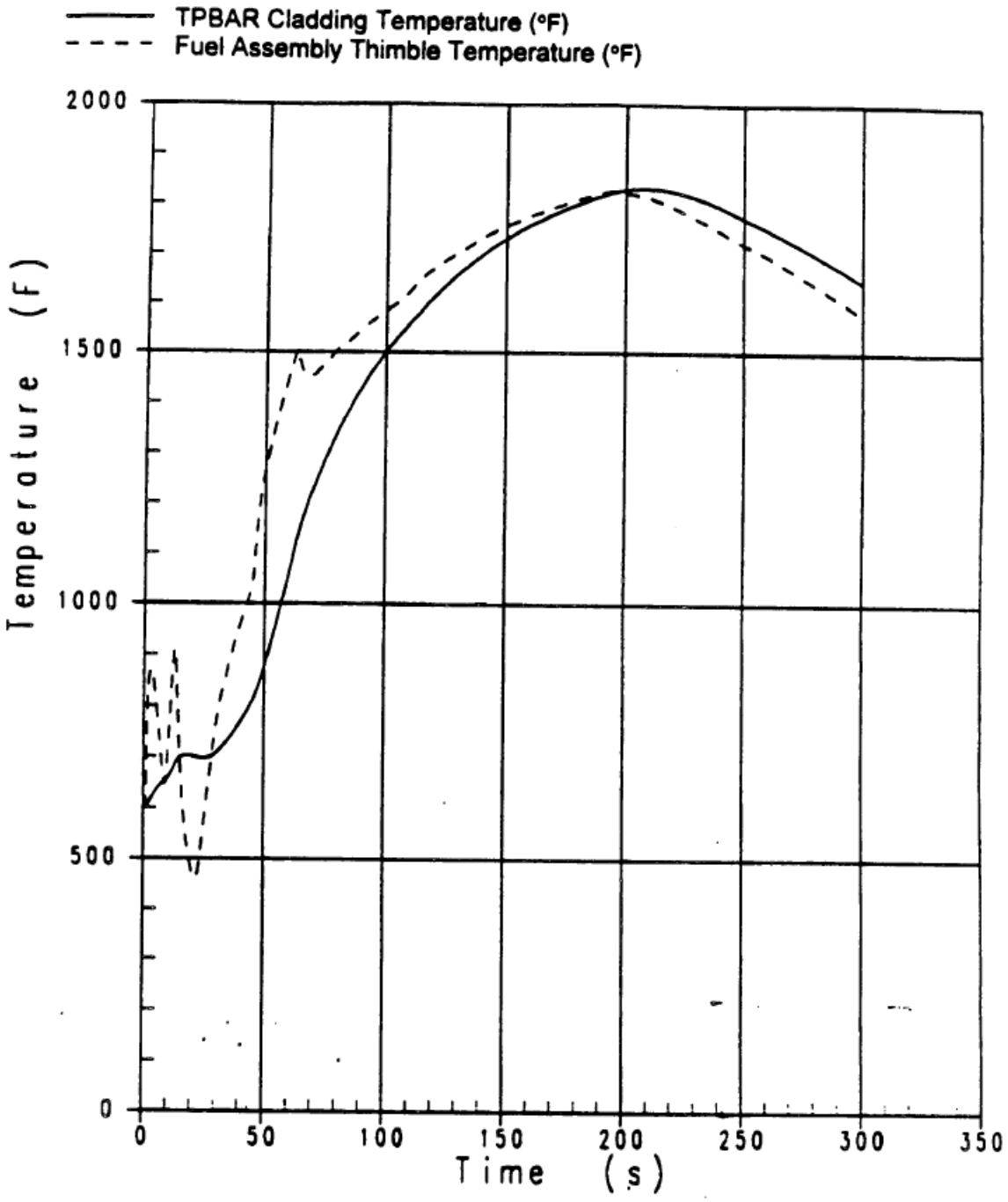

Figure 6: TPBAR LBLOCA response from Tritium Production Core Topical Report (Figure 2.15.5-1 of the TPC Report)

[a,c

]

Figure 7: TPBAR LBLOCA response from Tritium Production Core Topical Report (Figure 2.15.5-1 of the TPC report), with
[ ] a,c

[a,c

]

Figure 8: [ ]a,c

SFNB D-RAI 2

TVA has submitted a detailed analysis for high temperature failure model for TPBAR cladding during LOCA. TPBAR failure modes analyzed are the thermal creep rupture failure and rapid burst failure modes. For the thermal creep rupture and cladding burst failure analyses, provide responses to the following:

(a) Describe the five sets of experimental bursts tests performed by Pacific Northwest National Laboratory (PNNL). Describe how these experiments simulate the TPBAR thermal creep rupture failure.
(b) Describe the details of the cladding burst rupture model used in the TPBAR failure analysis.
(c) Provide details of the cladding creep rupture model and the procedure to develop the time to rupture curves.
(d) Describe how the burst and creep burst curves are used to determine the TPBAR failure assessment. The response should include the criteria to determine cladding failure.

TVA Response to SFNB D-RAI 2

The TPBAR cladding stresses during a LOCA event are calculated using classic elasticity theory and the development of stress intensities derived from American Society of Mechanical Boiler & Pressure Vessel Code (ASME-BPVC) methods. The allowable stress limits for TPBARs are evaluated by two mechanisms of stress-induced cladding failure. The first stress limit focuses on the condition that over-pressurization will lead to a rapid deformation process, commonly called burst rupture. Once the cladding stresses (as defined by the stress intensity) exceed a certain stress value, the material will rapidly fail by plastic deformation. The second allowable stress limit is concerned with the process of thermal creep rupture, which is a time-dependent mechanism of material deformation that leads to ductility exhaustion. The thermal creep rupture process is normally characterized by a time to rupture (or failure) parameter that is defined as a function of stress and temperature.

The burst rupture and creep models are treated separately but are related. Burst rupture occurs when the stress level exceeds the ultimate tensile strength, or when the creep transitions from primary to tertiary creep (essentially flow) without slowing to a secondary or steady creep rate. The creep rupture model assumes some time in steady-stated or secondary creep at stresses below ultimate tensile strength (UTS) and in most cases below yield strength (YS). Separate burst and creep rupture experiments have been performed by Hanford Engineering Development Laboratory (HEDL) and PNNL. The burst and creep rupture experiments are discussed in this response to SFNB D-RAI 2(a), while the burst and creep rupture models are discussed in the responses to SFNB D-RAI 2(b) and 2(c), respectively.

TVA Response to SFNB D-RAI 2(a)

The TPBAR transient temperature sequence during a LOCA consists of three regimes, 1) a heating period (approximately 10 to 100°F/sec), 2) a period of quasi-steady temperature lasting 30 to 600 seconds, and 3) a cooling period. High temperature test data have been used to establish the burst stress as a function of temperature. The five sets of experimental bursts

tests performed by PNNL were developed to establish the allowable stress limits for the first two of these regimes. PNNL has a burst model (curve) for 316 stainless steel tubing from the HEDL program and has used open literature data published by the program earlier testing performed by the HEDL program. To ensure that the burst model is valid for current cladding material, PNNL has performed experiments to complement those performed earlier in the program. The following describes the five data sets.

Burst experiments

In the burst tests, short cladding specimens were fitted with one solid end plug and one open end plug connected to a gas pressurization system; full-length specimens were pre-pressurized and sealed prior to testing. Typically, short specimens were heated to burst, while the full-length specimens were heated to a constant temperature and pressure until rupture. The cladding stress at rupture is calculated from the maximum pressure and the cladding dimensions using the thick-wall approximation. The temperatures and pressures used in these tests were based on LOCA analyses performed for nuclear reactor systems expected to host TPBARs.

In the case of the burst curve, because the specimen is pressurized (with a temperature ramp) to rupture, time is not used. Instead stress (at rupture) as a function of temperature is used. The burst stress is greater than UTS, which is a relatively high stress with respect to a given material, which normally operates below YS.

PNNL conducted five sets of burst test experiment as follows (summarized in TTP-3-721, Revision 1):

1. M. A. McKinnon (1992), PNNL Test #1a and Test #1b,
2. M. A. McKinnon (2002), PNNL Test #2,
3. D. E. Blahnik (2009), PNNL Test #3,
4. S. G. Pitman (2011), PNNL Test #4, and
5. S. G. Pitman (2016), PNNL Test #5.

The first PNNL Test was conducted on a preliminary TPBAR design for proof of concept. Short (4.4 inches) test specimens were constructed from 20 percent (%) cold-worked 316 stainless steel cladding. Eight specimens used coated cladding [0.0005 inch on outer diameter (OD), 0.002 inch on inner diameter (ID)], and another eight used uncoated cladding. The study was extended in Test #1b using four coated cladding specimens of 4-foot length containing one-foot pencils (sections of getter and pellets). In both experiments, the cladding was an earlier prototype (0.370 inch OD, 0.330 inch ID).

In each test for Test #1a, the specimen was charged with helium gas (target pressures were 1300, 2300, 3800, and 5500 psig) and then inductively heated to the point of bursting; ramp rates of 5.6 degrees Centigrade (°C)/sec (10°F/sec) were achieved in the heating process. The temperature at burst decreased with increasing pressure. The cladding temperatures were recorded by thermocouples and the pressure is monitored during the test. The burst tests were performed in air.

In Test #1b, four-foot long test conducted at four different backfill pressure with helium from 1000 psia to 3000 psia and inductively heated at a rate of 5.6°C/s (10°F/s) until burst. The primary objective of this study was to determine whether pellet relocation is confined to the pencil at the burst location when the pencils are of prototypic length. Another motivation was to use prototypic hardware and longer cladding tubes.

Tests #2 and #3 involved full-length specimens of 20% cold-worked stainless steel 316 cladding containing prototype hardware (getters, pellets, liners) in order to test the response of prototype TPBARs under LOCA temperatures. The objective of the TPBAR burst testing was to determine the amount of pellet material ejected from a full-length TPBAR under prototypic nuclear power reactor LBLOCA conditions with high temperature and high rod internal pressure levels.

In Test #2, the test articles were pressurized with helium and heated until they burst, with pressures at approximately 2600, 3300, and 4000 psi, and temperatures from 1700 to 1780°F. Seven tests were conducted. The system temperature was brought to 800°F, then the temperature was ramped to 1800°F over a period of six minutes followed by a hold at temperature until rupture.

Four additional full-length TPBAR burst tests were conducted in Test #3 representing four TPBAR designs [including Mark 8 multi-pencil, Mark 9.1 full-length getter (FLG), Mark 8.1 multi-pencil, and Mark 9.2 FLG designs]. The TPBAR test was initiated by starting the data recording and then bringing the temperature of the heater rods to 800°F. This was achieved by ramping power to the heater rods linearly over a 40-second time period to an output of 20 kilowatts (kW). Once the heater rods achieved the target value of 800°F, the power was reduced to four kW and held at that level for 30 minutes (1800 seconds) to allow the heat to distribute evenly through the facility and to allow the middle of the heated length (MOHL) of the test rod to reach 800°F. Next, the power was ramped up linearly over a 10-second time period to a high power output of 70 kW and held at that level until the test bundle maximum temperature was 1800°F (the desired result was to quickly bring up the heater-rod temperatures to near 1800°F).

The fourth and fifth tests (Tests #4 and #5) were performed at PNNL. The test articles used short lengths (approximately seven inches) of coated cladding with a hollow stainless steel filler rod to limit the gas volume. Each test specimen had five thermocouples attached to the outer surface at intervals of 0.5 inch to monitor the cladding temperature, and the threaded hollow lower end fitting allowed the test specimen to be attached to a monitored pressurization system. The specimen was pressurized with helium to approximately 1500 psig, then brought to a preset level of at least 2000 psig. During the heating cycle, the pressure and the five temperature readings were recorded. The temperature of the cladding was brought to 500°F, held for a brief period, and ultimately ramped until the specimen burst. The controller continued through initial heat-up, soak, and ramp stages. After the specimen burst, the heating power was shut down and the specimen was allowed to cool.

In the fourth experiment, nine tests [three specimens at three temperatures (1450°F, 1600°F and 1900°F)] were performed.

Each burst test was considered acceptable if 1) the overall temperature ramp rate was held to the required limits; 2) the temperature and pressure time histories were recorded; 3) the information was recorded on the test data sheet; 4) the specimen's temperature was increased until the specimen had burst; and 5) burst appearance was typical of expected ruptures for similar test articles. In addition, the burst tip must have been at least five diameters away from the end plug or high-pressure fitting.

In the fifth experiment, 14 sets of tests of 61 specimens were completed as shown in Table 2a-1 and are discussed below.

Table 2a-1: PNNL Burst Tests

Test Config.	Temperature, °F	Target Ramp Rate, °F/s (°C/s)	Soak Temperature, °F / Time	Number of tests
A1	1300	10 (5.6)	500°F, 300 s	9
A2	1600			10
A3	1900			9
A4	1490			3
A5	1690			3
B1	1300	3 (1.7)		3
B2	1490			3
B3	1690			3
C1	1300	16 (9)		3
C2	1490			3
C3	1690			3
D1	1300	10 (5.6)	800°F, 26 min	3
D2	1490			3
D3	1690			3

Creep Rupture Experiments

Pressurized cladding (tubing) creep rupture tests were conducted with at least four pressures at six different cladding temperatures: 1500°F, 1525°F, 1550°F, 1575°F, 1600°F and 1625°F, which span the likely maximum temperature achieved by TPBARs during a LBLOCA event. Each specimen was pressurized at room temperature in atmospheric conditions to a predetermined level, then the temperature was ramped (at a rate of 20°C/s) to the test temperature, and then the pressure and temperature were held constant until rupture. The specimen underwent a steady creep rate, then ruptured in the last several seconds at increasing strain rates (tertiary creep or flow).

PNNL conducted 98 tests used for the development of a creep rupture model. The tests were conducted in three groups (series). The initial test series (500 series) encompassed 48 tests, with four testing temperatures (1525, 1550, 1575, and 1600°F). Three tests (triplicate) were performed at the same target internal pressure for each target temperature.

A second set of tests (600 series) were performed at the same four test temperatures. Some tests were repeats of tests in the 500 series, while others introduced new pressures to expand

the range of test conditions. Finally, a third set of tests (700 series) expanded the temperature range by adding tests at 1500 and 1625°F.

For each test, the pressure was converted to stress, and with the temperature and time to failure, the results were evaluated using the Larson-Miller parameter and Life Fraction Rule (see response to SFNB D-RAI 2(c)). The life fraction was set to unity corresponding to the failure time, and each test gives a unique C-value. The ruptures tended to occur near the peak temperature location, and the geometries of the bursts were classified into five types and compared for consistency and trends. In one final test, a specimen was heated for multiple periods of approximately 120 seconds. The cladding outer diameter was measured in two perpendicular orientations at the thermocouple locations, and an average strain rate was determined. The strains and strain rates (on the order of 10^{-4} s^{-1}) show a uniform behavior through the steady state creep portion of the test. The transition to tertiary creep rates was observed during the later times in the tests.

TVA Response to SFNB D-RAI 2(b)

A high temperature cladding burst rupture model was developed specific to TPBAR cladding material using experimental data from both open literature testing on cold-worked stainless steel 316 and from tests performed by PNNL on TPBAR coated cladding samples. Heating of the TPBARs during an LBLOCA event can result in rupture of the TPBAR cladding due to the increase in internal pressure, the decrease in external pressure, and the decrease in cladding strength at high temperature. For a given temperature, burst rupture will occur by plastic deformation as the differential pressure increases to exceed the stress intensity allowable limit. The TPBAR burst rupture model has been developed to predict cladding rupture given a set of pressure and temperature conditions seen during a transient.

The cladding burst rupture model to calculate the probability for TPBAR cladding mechanical rupture in a LBLOCA event uses a 95/95 lower one-sided tolerance for the experimentally measured burst stress. The burst stresses were calculated using the thick-walled hoop stress with nominal cladding inner and outer radius for uncoated cladding tubes. This approach is consistent with the assumption used to calculate the stress intensities from the applied loads.

The formula of the thick-walled hoop stress is given as:

$$\sigma = P\frac{(R_{Outer}^2 + R_{Inner}^2)}{(R_{Outer}^2 - R_{Inner}^2)}$$

Where;

σ is thick-walled hoop stress,
P is the highest gage pressure measured at burst,
R_{Inner} is the nominal cladding inner tube radius, and
R_{Outer} is the nominal cladding outer tube radius.

The burst pressure measurements from the experimental data described in SFNB D-RAI 2(a) were converted to the thick-walled burst stress and correlated with temperature at burst.

The TPBAR burst stress model was obtained by performing a data fitting operation with a seventh order polynomial expression to relate the measured thick-walled hoop stress at burst to the applied cladding temperature.
The result is given by:

$$\sigma_{burst}(T) = A + B \cdot T + C \cdot T^2 + D \cdot T^3 + E \cdot T^4 + F \cdot T^5 + G \cdot T^6 + H \cdot T^7$$

where σ_{burst} is the thick wall hoop stress at rupture in *ksi* and *T* is the temperature in °F. Two sets of polynomial coefficients were developed: best-estimate (BE) and 95/95 lower bound (LB). These coefficients are provided in Table 2b-1.

Table 2b-1 Polynomial Coefficients for the LB and BE Burst Stress Model[1]

95/95 LB	Value	BE	Value
A_{LB}	-1.2182110E+01	A_{BE}	7.4662840E+01
B_{LB}	7.4381080E-01	B_{BE}	1.9886980E-01
C_{LB}	-1.9142010E-03	C_{BE}	-3.9085080E-04
D_{LB}	2.5960540E-06	D_{BE}	4.1774550E-07
E_{LB}	-2.0691570E-09	E_{BE}	-3.3221110E-10
F_{LB}	9.4271060E-13	F_{BE}	1.5945130E-13
G_{LB}	-2.2702770E-16	G_{BE}	-3.9965480E-17
H_{LB}	2.2521420E-20	H_{BE}	4.1222410E-21

The lower bound thick-wall hoop burst curve has been selected as the allowable stress limit for evaluation of the primary membrane stress intensity factor of safety. The polynomial expression coefficients for burst stress model are applicable in the temperature range of 500°F to 2000°F. The thick-wall hoop burst stress at temperatures below 500°F uses the 500°F value, which ensures complete coverage across the range of applicability for the stress analysis.

TVA Response to SFNB D-RAI 2(c)

The high temperature strength of TPBAR stainless steel coated cladding can lead to time dependent deformations at applied stress conditions below the burst stress during the quasi-steady state temperature regime of a LOCA event. Material failure by this process is called thermal creep rupture, the assessment of which requires a model that considers the time dependent temperature and pressure conditions during a LOCA.

To calculate the conditions leading to failure under time-varying stress and temperature conditions, PNNL has developed a thermal creep rupture model using data available in the open literature for cold-worked stainless steel 316 and from thermal creep tests performed by PNNL on TPBAR coated cladding material. The outcome is a thermal creep rupture model that calculates the accumulation of time dependent material damage using the applied cladding stress and temperature conditions. A conservative approach was used to ensure that the

[1] These coefficients will yield a thick-wall hoop stress in ksi. The temperature used is in °F.

thermal creep rupture model does not overpredict the time to failure when used in the LOCA calculations. The following describes the approach used to derive the TPBAR coated cladding thermal creep rupture model.

Mechanical property tests have been performed on relevant stainless steel (SS) cladding material as part of the development of fast test reactor fuel cladding comprised of 20% cold-worked SS 316 (References 2c.1 and 2c.2). These tests include uniaxial tensile, burst, stress rupture, and thermal transient loading procedures to provide information on strength (yield and failure stress) and strain to failure.

Straalsund et al. (Reference 2c.1) and Johnson (Reference 2c.2) used their data to evaluate the use of the Larson-Miller parameter (LMP) with the life fraction (LF) rule in order to correlate the rupture time with the rupture temperature and stress. In their work, a fifth-degree polynomial for the LMP as a function of modulus modified stress was developed as:

$$LMP = \left(A_{lmp} + B_{lmp}\sigma_m + C_{lmp}\sigma_m^2 + D_{lmp}\sigma_m^3 + E_{lmp}\sigma_m^4 + F_{lmp}\sigma_m^5\right)10^4 \quad \text{(2c-1)}$$

Where;

$\sigma_m =$ modulus modified stress
$A_{lmp} = 4.862$
$B_{lmp} = -7.782 \times 10^{-2}$
$C_{lmp} = 2.458 \times 10^{-3}$
$D_{lmp} = -4.862 \times 10^{-5}$
$E_{lmp} = 4.746 \times 10^{-7}$
$F_{lmp} = -1.865 \times 10^{-9}$

The modulus modified stress is defined as:

$$\sigma_m = \sigma_T \, E_{1400}/E_T \quad \text{(2c-2)}$$

Where;

$\sigma_T =$ stress at temperature T [°F]
$E_T =$ elastic modulus at temperature
$E_{1400} =$ elastic modulus at 1400[°F]

LMP is given as:

$$LMP = T[log_{10}(t_r) + C] \quad \text{(2c-3)}$$

Where;

$T =$ absolute temperature [°R]
$t_r =$ time − to − rupture [hours]
$C =$ material constant [20 in open literature]

and the LF rule is given as

$$LF = \int_0^{t^*} \left[t_r\left(\sigma(t), T(t)\right)\right]^{-1} dt = 1 \quad \text{(2c-4)}$$

Where;

$t =$ time
$t^* =$ failure time
$t_r\left(\sigma(t), T(t)\right) =$ stress − rupture life of material
$\sigma(t) =$ stress
$T(t) =$ temperature

The thick-walled hoop stress arising from the pressure load was used for the stress controlling the thermal creep rupture and is given as

$$\sigma_T = P\,(R_{Outer}^2 + R_{Inner}^2)/(R_{Outer}^2 - R_{Inner}^2) \quad \text{(2c-5)}$$

Where;

$P =$ gage pressure measured at the burst testing
$R_{Inner} =$ inner cladding radius
$R_{Outer} =$ outer cladding radius

To supplement the open literature data, PNNL conducted pressurized biaxial thermal creep tests to generate time-to-failure data for TPBAR coated cladding for the expected range of possible temperature and pressure levels representative of a LOCA event. These tests were performed over a temperature range between 1500°F and 1625°F with rupture times that varied from 50 to 2850 seconds.

A TPBAR cladding specific *C*-parameter was derived from these tests for use in the creep damage model. The *C* parameter for each experiment performed by PNNL was calculated using the Straaslund and Johnson functional model for the Larson Miller Parameter (Equation 2c-1), the Larson-Miller model (Equation 2c-3) and the life fraction rule (Equation 2c-4). A numerical iteration approach was applied to yield the *C*-parameter for each test specimen. The test specimen specific *C*-parameters were combined to yield a best-estimate (*C* = 19.653 +/- 0.0906) specific to TPBAR cladding.

To implement the Larson-Miller model into the TPBAR stress analysis methodology, an approach was developed based on a discrete set of time-to-rupture curves as a function of applied stress and temperature. This type of approach was required in order to be consistent with the method selected to calculate the primary membrane stress intensity for the applied loads during a LOCA.

A total of five time-to-rupture values (t_r) used were 60, 120, 300, 600 and 1200 seconds and temperatures ranged from 500 to 1800°F to span the expected conditions. The procedure to develop each of the constant time-to-rupture curves is as follows;

1. For a time to rupture (e.g., t_r = 60 seconds), calculate the LMP using Equation 2c-3 with $C = 19.653$ at discrete temperatures between 500°F and 1800°F.

2. Determine the modulus modified stress for each LMP by using a root-solving technique: namely the computation of $\sigma_m = f^{-1}(LMP)$ with the fifth-degree polynomial for the LMP vs. modulus modified stress correlation (Equation 2c-1).
3. Calculate the thick-wall hoop stress (σ_T) from the modulus modified stress (σ_m) using Equation 2c-2.
4. Using the tabular data of thick-wall hoop stress at discrete temperatures, obtain a fifth degree polynomial for the thick-wall hoop stress (σ_T) versus temperature curve.

Once the best estimate thick-wall hoop stress as a function of temperature was created for each of the five discrete time-to-rupture values, a statistical approach was applied to develop a 95/95 tolerance lower bound curve. Standard first order propagation of error was used to consider the uncertainties in the LMP data from the open literature, the variability in the PNNL tests, and the methodology used to derive the curves.

Table 2c-1 provides the polynomial coefficients for the 95/95 lower bound stress curves as a function of temperature for each of the constant time-to-rupture values (t_r), from which a thermal creep rupture model of fifth degree polynomials was obtained as:

$$\sigma_{\frac{95}{95}}^{t_r} = A_{\frac{95}{95}}^{t_r} + B_{\frac{95}{95}}^{t_r} T + C_{\frac{95}{95}}^{t_r} T^2 + D_{\frac{95}{95}}^{t_r} T^3 + E_{\frac{95}{95}}^{t_r} T^4 + F_{\frac{95}{95}}^{t_r} T^5 \qquad \text{(2c-6)}$$

where

$t_r =$ constant time to rupture values of $60, 120, 300, 600$ and 1200 seconds
$T =$ temperatures $(1000\ [^{\circ}\mathrm{F}] \leq T \leq 1800\ [^{\circ}\mathrm{F}])$
$\sigma_{\frac{95}{95}}^{t_r} =$ stresses [ksi] of the $95/95$ tolerance lower bounds

Table 2c-1 Coefficients $\boldsymbol{A_{\frac{95}{95}}^{t_r}, B_{\frac{95}{95}}^{t_r}, C_{\frac{95}{95}}^{t_r}, D_{\frac{95}{95}}^{t_r}, E_{\frac{95}{95}}^{t_r}}$, and $\boldsymbol{F_{\frac{95}{95}}^{t_r}}$ for Equation 2c-6

	t_r = 60 [s]	t_r = 120 [s]	t_r = 300 [s]	t_r = 600 [s]	t_r = 1200 [s]
$A_{\frac{95}{95}}^{t_r}$	-3.006350E+02	7.054940E+02	1.895800E+03	2.565630E+03	2.947790E+03
$B_{\frac{95}{95}}^{t_r}$	1.874410E+00	-1.858010E+00	-6.375040E+00	-8.994120E+00	-1.057510E+01
$C_{\frac{95}{95}}^{t_r}$	-3.097270E-03	2.379470E-03	9.157900E-03	1.320340E-02	1.577360E-02
$D_{\frac{95}{95}}^{t_r}$	2.433530E-06	-1.542780E-06	-6.574870E-06	-9.663910E-06	-1.172150E-05
$E_{\frac{95}{95}}^{t_r}$	-9.653450E-10	4.609030E-10	2.305710E-09	3.469040E-09	4.277630E-09
$F_{\frac{95}{95}}^{t_r}$	1.543160E-13	-4.766370E-14	-3.145370E-13	-4.871290E-13	-6.116960E-13

The application of the time to rupture curves described in Equation 2c-6 to calculate the potential for creep rupture in TPBARs requires consideration that the thick-walled hoop stress and temperature vary with time during a LOCA event. The time variation of the stress and temperature conditions are accounted for using a damage accumulation model based on the life fraction rule. As shown in Equation 2c-4, the life fraction rule integrates that amount of time

exposed for a given time to failure. For example, using a discretized form of Equation 2c-4, the life fraction model yields 0.5 when the temperature and stress conditions are constant for 60 seconds at the 120-second rupture time curve, as shown in equation 2c-7.

$$\frac{\Delta t}{t_r} = \frac{60s}{120s} = 0.5 \tag{2c-7}$$

Failure is expected to occur by creep rupture when the life fraction model reaches unity. For the discrete model developed for the TPBAR stress analysis, the life fraction (LF) approach reduces to:

$$LF = \frac{t_{1200}}{1200\ s} + \frac{t_{600}}{600\ s} + \frac{t_{300}}{300\ s} + \frac{t_{120}}{120\ s} + \frac{t_{60}}{60\ s} \tag{2c-8}$$

where;

t_{60} = the total time(s) when the stress conditions exceed the 60 second rupture curve
t_{120} = the total time(s) when the stress conditions exceed the 120 second rupture curve and are below the 60 second rupture curve.
t_{300} = the total time(s) when the stress conditions exceed the 300 second rupture curve and are below the 120 second rupture curve.
t_{600} = the total time(s) when the stress conditions exceed the 600 second rupture curve and are below the 300 second rupture curve.
t_{1200} = the total time(s) when the stress conditions exceed the 1200 second rupture curve and are below the 600 second rupture curve.

Figure 2c-1 is a simplification to illustrate the approach used to implement the creep rupture model. In the case of actual LOCA conditions, the model considers the time variation of both the applied stress and temperature in the calculation of the life fraction.

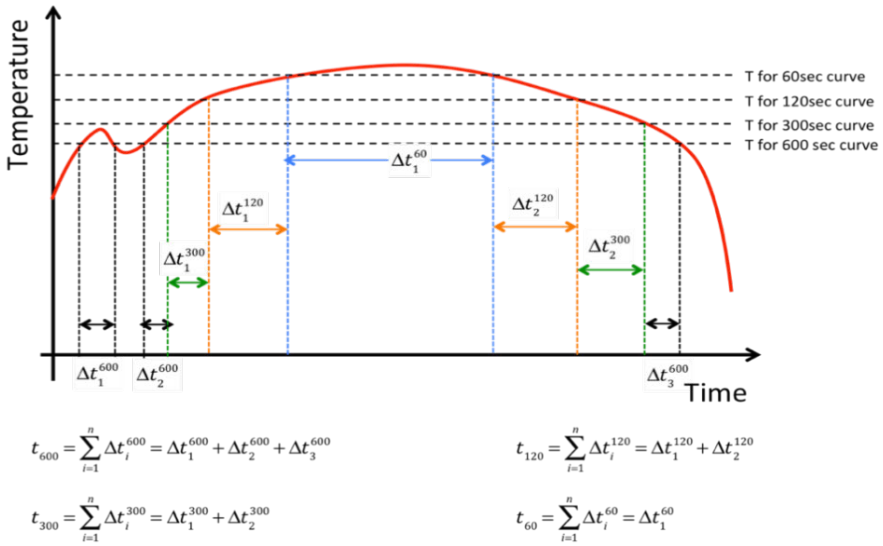

Figure 2c-1: Simplified Diagram of Temperatures Seen During a LOCA

Comparison of the discrete model shown above, and a continuous integration of the life fraction rule, finds that in certain conditions, the discrete model can under-predict the life fraction. To account for the potential for an under-prediction of the life fraction, a factor of 2 has been applied in the TPBAR stress analysis approach.

References

2c.1 Straalsund, J.L., R.L. Fish and G.D. Johnson, "Correlation of Transient-Test Data with Conventional Mechanical Properties Data," Nuclear Technology, Vol. 25, pp. 531-540, 1975

2c.2 Johnson, G. D., "Evaluation of Mechanical Properties with the Larson-Miller Parameter," HEDL-TME 75-33, April 1975

TVA Response to SFNB D-RAI 2(d)

The burst rupture and creep rupture curves are the allowable stress limits for TPBAR behavior during a LOCA event. They represent the stress limits for burst rupture and thermal creep rupture mechanisms. The cladding stresses are calculated using classic elasticity theory and the development of stress intensities derived from ASME-BPVC methods. These stress intensities are then compared to actual burst and creep burst curves at TPBAR temperature and axial location to generate the smallest factor of safety.

The stress intensities arising from the imposed forces are compared to the allowable stress limits obtained from the experimentally determined burst and thermal creep rupture curves. In the case of TPBAR cladding burst failure, the approach compares the calculated stress intensities against the allowable burst stress limit to determine the minimum factor of safety.

The factor of safety for TPBAR cladding burst during LOCA conditions is calculated from:

$$FS = \frac{(Lower\ bound\ burst\ allowable\ stress)}{(stress\ intensity)}$$

The structural integrity of the TPBAR is evaluated by comparing the factor of safety to a value of unity. Failure is expected for FS < 1.0.

In the case of TPBAR cladding failure by creep rupture, the stress intensity is used in a cumulative creep damage model to calculate the factor of safety. As described in the response to SFNB D-RAI 2(c), the time to cladding failure is calculated using the cladding stress intensity along with a set of time to failure curves. The creep rupture damage accumulation model is composed of five curves that relate the cladding applied stress and temperature to the time required to rupture the cladding.

These five curves represent discrete times to failure at 60, 120, 300, 600, and 1200 seconds. The life fraction rule is applied to compute the accumulation of damage caused by creep mechanisms for conditions when the stress intensity exceeds the creep rupture curves. The accumulated creep damage (D) is then used to assess the potential for failure by the creep rupture mechanism using the following criteria.

D < 1.0 creep rupture not expected
D ≥ 1.0 creep rupture expected

The creep damage allowable limit is applied only to the primary membrane plus bending stress intensities as these stress components are the extended long time applied stresses during the event.

The equations above step through the elastic stress solutions and how the methodology of the ASME Code Section III-NG combines these stresses to generate primary and secondary code stress intensities. The most conservative stress intensities are then compared to actual experimental data corresponding to TPBAR temperature and axial location to generate the smallest factor of safety in the TPBAR.

SFNB D-RAI 3

TVA states that a statistical approach similar to the that used in FSLOCA Evaluation Model to demonstrate compliance with 10 CFR 50.46 acceptance criteria is used for the LOCA-specific TPBAR stress analysis. The figures-of-merit (FOM) are related to (1) rupture due to primary and bending stress and (2) rupture due to creep damage. Provide the following information related to stress evaluation metric that is capable of directly processing results from FSLOCA analysis:

(a) Provide a list of input parameters and derived parameters that are used in the calculation of stress intensities. Also list the assumptions and range of validity for the metric.
(b) Describe the primary and secondary stresses and their components that are considered in the development of the TPBAR structural model.

(c) Explain how the stress intensities are derived based on the American Society of Mechanical Engineers Boiler and Pressure Vessel Code, Section III, Subsection NG.
(d) Describe how allowable stress limits are calculated for burst stress, end plug stress, and creep damage stress. Provide justification for the selection of allowable stress that results in TPBAR stress failure.

TVA Response to SFNB D-RAI 3(a)

The input parameters used in the calculation of the TPBAR cladding stress intensities are listed in Table 3a-1 and the derived parameters are listed in Table 3a-2.

Table 3a-1: Input Parameters

Input Parameter	Value
Internal void volume	6.5 in^3
Cladding inner diameter (nominal)	0.336 in
Cladding outer diameter (nominal)	0.381 in
Maximum outer surface corrosion layer thickness	0.000124 in
Cladding diameter fabrication tolerance	0.0005 in
Guide thimble tube inner diameter (maximum)	[ ]a,c
Length of dashpot region (maximum)	[ ] a,c
Length of trimmed cladding	150.726 in

Table 3a-2: Derived Parameters

Variable	Description	Value	Calculation Comments
R_i	maximum cladding inner radius $\frac{D_i + \Delta}{2} + \epsilon$	Calculated	Nominal inner cladding radius (D_i) fabrication tolerance (Δ) corrosion thickness (ϵ)
R_o	minimum cladding outer radius $\frac{D_o - \Delta}{2} - \epsilon$	Calculated	Nominal outer cladding radius (D_o) fabrication tolerance (Δ) corrosion thickness (ϵ)
R_m	mean radius $(R_o + R_i)/2$	Calculated	Max cladding inner radius Min cladding outer radius
t_w	minimum cladding wall thickness $R_o - R_i$	Calculated	Max cladding inner radius, Min cladding outer radius
P_i	internal rod pressure	Variable psi	Temperature and volume
P_o	outer ambient pressure	14.7 psi	Assumed RCS pressure
ΔP	Pressure differential $P_o - P_i$	Variable psi	Internal rod pressure minus outer ambient pressure
δ_{max}	Maximum lateral deflection $G_{ID} - 2 \cdot R_o$	Calculated	Guide tube maximum ID cladding minimum OD

Assumptions and Range of Validity for the Metric

- The TPBAR cladding axial temperature profile is set equal to the hot assembly peak fuel rod axial cladding temperature profile. This assumption overestimates the actual TPBAR temperature (both maximum and volumetric average) for two reasons: 1) the initial TPBAR stored energy is lower than a fuel rod and 2) radiative heating from the surrounding fuel rods delay the heat up of the TPBARs relative to the temperature experienced by the peak fuel rod.
- The reactor coolant system (RCS) pressure is set equal to 14.7 psia for the entire duration of the LOCA event to maximize the stress arising from the internal rod pressure. This value is conservative because during a LBLOCA and post-LBLOCA the RCS pressure drops rapidly, but cannot drop below ambient pressure (i.e., 14.7 psia).

The polynomial expressions used in the TPBAR LOCA metric are applicable for the temperature range between 200°F and 1900°F and tritium production levels up to 1.5 grams per rod. (TPBARs are assumed to fail for cladding temperatures greater than 1900°F due to the lack of experimental data above these temperatures.)

TVA Response to SFNB D-RAI 3(b)

The stress field on the TPBAR is evaluated using a methodology based on the ASME-BPVC approach, including calculations for the primary membrane stresses (P_m), the primary bending stresses (P_b), as well as secondary stresses (P_q). Two secondary stress components are considered: the thermal stresses due to the radial temperature gradient across the cladding and the stresses caused by the geometrical discontinuity represented by the end-plug and cladding interface.

The analytical approach follows the intent of the ASME Code Section III-NB and addresses primary and secondary stress contributions. Primary stresses include TPBAR stress components due to internal pressure, rod ovality, and lateral deflections. Secondary stresses include stresses due to cladding quench and end plug-wall discontinuity stress. Using the ASME-BPVC approach to combine the stress intensities in the calculation of the factor of safety effectively reduces the stress intensity to a conservative estimate of the hoop stress in the TPBAR. The hoop stress is then compared to experimentally measured failure data under representative temperature and stress conditions.

The primary and secondary stress components considered in the development of the TPBAR structural model are described below.

Primary Membrane and Bending Stresses

- *Stresses induced by internal rod pressure*: radial, tangential, and axial, along with their mean values are calculated using the thick-wall pressure vessel Lame' equations. The ASME Code approach is used to compute the maximum absolute values from these equations for each orthogonal direction.
- *Axial bending stresses due to lateral deflections*: axial membrane stresses in the cladding induced as a result of rod bending in the fuel assembly guide tube. Stresses are calculated by application of the beam bending flexure equation.

Secondary Stresses

- *Thermal stresses*: secondary stresses induced by the radial temperature gradient across the cladding wall caused by in-reactor quench cooling.
- *End plug discontinuity stresses*: stresses induced in the cladding region close to the end-plug due to the effects of a pressurized capped tube. (These are equations for a pressurized shell with fixed ends)

In the application of the TPBAR stress analysis methodology to LBLOCA conditions, the secondary stresses arising from the radial temperature gradient across the cladding wall and the end-plug stress discontinuity were found to be non-limiting. As such, contribution of the secondary stresses in the TPBAR structural integrity evaluations was removed from consideration.

TVA Response to SFNB D-RAI 3(c)

The analytical approach used to calculate the stress intensity is derived from the ASME Code Section III-NG and addresses primary and secondary stress contributions and the subsequent stress intensity combinations. The maximum of these ASME-BPVC combinations, which is additionally reduced to a conservative estimate of the TPBAR hoop stress, is then compared to actual allowable stress limits based on experimental data developed under representative temperature conditions for generation of the smallest factor of safety.

The TPBAR cladding stress components are separated into primary membrane stresses, primary bending stresses, and secondary stresses. As discussed in the response to SFNB D-RAI 3(b), the applied loads to a TPBAR during a LOCA are captured within these categories. The stress intensities for each category are evaluated based on the maximum absolute value of the stress tensor; adding the absolute sum of the stress differences and then selecting the maximum to define the stress intensities is conservative because they are positive-definite quantities.

The derivations below summarize the method for combining stress components into the stress intensities in each category and identification of the maximum stress intensity for use in the factor of safety calculation (see Tables 3c-1 and 3c-2 for definition of variables). *S* variables represent the ASME code nomenclature and the σ variables representing classic elasticity nomenclature. The cladding stress components are calculated using classic elasticity theory and the development of stress intensities derived from ASME-BPVC methods as shown below

The pressure stresses and axial membrane stress due to flow bending are considered for the primary membrane stress intensity.

$$\begin{aligned} Sm_1 &= \sigma_{tm} \\ Sm_2 &= \sigma_a + \sigma_{ab} \\ Sm_3 &= \sigma_{rm} \end{aligned} \qquad \text{(3c-1)}$$

The membrane stress intensities are then combined as follows:

$$\begin{aligned} Sm_{12} &= Sm_1 - Sm_2 = |\sigma_{tm} - \sigma_a| + |\sigma_{ab}| \\ Sm_{23} &= Sm_2 - Sm_3 = |\sigma_a - \sigma_{rm}| + |\sigma_{ab}| \\ Sm_{31} &= Sm_3 - Sm_1 = |\sigma_{rm} - \sigma_{tm}| \end{aligned} \quad \text{(3c-2)}$$

Therefore, the maximum primary membrane stress intensity is calculated:

$$SI_m = \max\{Sm_{12}, Sm_{23}, Sm_{31}\} \quad \text{(3c-3)}$$

The primary membrane stress intensity is combined into a primary membrane plus bending stress intensity as shown below:

$$SI_{mb} = SI_m + SI_b \quad \text{(3c-4)}$$

For the conditions of a LOCA event, where the inner rod pressure is greater than the external coolant pressure, the bending stress intensity (SI_b) from an oval cladding tube is equal to zero and this simplifies to the primary membrane stress intensity component:

$$SI_{mb} = SI_m \quad \text{(3c-5)}$$

For secondary stress intensities, the contributions from the thermal gradients across the cladding and the stress risers at the top end-plug region are separated. The calculation of the secondary stress intensity from thermal gradients is given from the approach.

$$\begin{aligned} Sq_1 &= \sigma_{tt}^o \\ Sq_2 &= \sigma_{tz}^o \\ Sq_3 &= 0 \end{aligned} \quad \text{(3c-6)}$$

The radial thermal stresses are identically equal to zero and that the tangential and axial stresses are equal at the outer and inner surfaces of the cladding. The secondary stress intensities are then combined;

$$\begin{aligned} Sq_{12} &= Sq_1 - Sq_2 = \sigma_{tt}^o - \sigma_{tz}^o = 0 \\ Sq_{23} &= Sq_2 - Sq_3 = \sigma_{tz}^o \\ Sq_{31} &= Sq_3 - Sq_1 = -\sigma_{tt}^o \end{aligned} \quad \text{(3c-7)}$$

Therefore, the secondary stress intensity due to thermal gradients is calculated as shown below:

$$SI_q = \max\{|Sq_{12}|, |Sq_{23}|, |Sq_{31}|\} \quad \text{(3c-8)}$$

The secondary stresses are then combined with the primary membrane plus bending stresses to yield the total primary plus secondary stress intensities:

$$SI_{mbq} = SI_{mb} + SI_q \quad \text{(3c-9)}$$

The secondary stresses due to the stress risers in the top end-plug region are evaluated and:

$$\begin{aligned} Sep_1 &= \sigma_{tc} \\ Sep_2 &= \sigma_{ac} \\ Sep_3 &= 0 \end{aligned} \quad \text{(3c-10)}$$

The secondary stress intensities for the end-plug region are then combined as follows:

$$\begin{aligned} Sep_{12} &= Sep_1 - Sep_2 = \sigma_{tc} - \sigma_{ac} \\ Sep_{23} &= Sep_2 - Sep_3 = \sigma_{ac} \\ Sep_{31} &= Sep_3 - Sep_1 = -\sigma_{tc} \end{aligned} \quad \text{(3c-11)}$$

Therefore, the secondary stress intensity at the end-plug region is calculated as follows:

$$SI_{ep} = \max\{|Sep_{12}|, |Sep_{23}|, |Sep_{31}|\} \quad \text{(3c-12)}$$

Classic elasticity equations/solutions were incorporated into the ASME code stress intensity definitions. These code primary and secondary stress intensities were defined and then reduced as determined by the specific TPBAR LOCA conditions. These stress intensities were then compared to actual experimentally determined allowable stress limits at TPBAR temperature and axial location to generate the smallest factor of safety.

Table 3c-1 ASME Stress Intensity Evaluation Variables

Variable	Definition
Sm_1	primary membrane stress intensity = mean surface tangential stress
Sm_2	primary membrane stress intensity = mean axial stress + axial stresses (lateral deflection)
Sm_3	primary membrane stress intensity = mean surface radial stress
Sm_{12}	combining membrane stress intensities
Sm_{23}	combining membrane stress intensities
Sm_{31}	combining membrane stress intensities
SI_m	maximum primary membrane stress intensity
SI_{mb}	primary membrane plus bending stress intensity
SI_b	bending stress intensity (ovality identically zero for LOCA)
Sq_1	secondary stress intensity from thermal gradients = outer surface tangential stress (quench)
Sq_2	secondary stress intensity from thermal gradients = outer surface axial stress (quench)
Sq_3	secondary stress intensity from thermal gradients
Sq_{12}	combining secondary stress intensities
Sq_{23}	combining secondary stress intensities
Sq_{31}	combining secondary stress intensities
SI_q	secondary stress intensity due to thermal gradients
SI_{mbq}	total primary (SI_{mb}) plus secondary stress (SI_q)intensities
Sep_1	secondary stresses due to the stress risers = maximum tangential stress (end plug)
Sep_2	secondary stresses due to the stress risers = maximum axial stress (end plug)
Sep_3	secondary stresses due to the stress risers
Sep_{12}	combining secondary stress intensities
Sep_{23}	combining secondary stress intensities
Sep_{31}	combining secondary stress intensities
SI_{ep}	secondary stress intensity at the end-plug region
SI_{mb}	primary membrane plus bending stress intensity

Table 3c-2 Greek Symbols

Variable	Definition
σ_{rm}	mean surface radial stress
σ_{tm}	mean surface tangential stress
σ_a	mean axial stress
σ_{ab}	axial stresses (lateral deflection)
σ_{tt}^o	outer surface tangential stress (quench)
σ_{tz}^o	outer surface axial stress (quench)
σ_{th}	tangential stress (end plug)
σ_{ac}	maximum axial stress (end plug)
σ_{tc}	maximum tangential stress (end plug)

TVA Response to SFNB D-RAI 3(d)

Allowable Stress Limits

The allowable limits for burst stress and creep damage evaluation are calculated using models derived from experimental data over a temperature of range of 500°F to 2000°F, and applied hoop stresses ranging from approximately 10 ksi to approximately 100 ksi. The allowable stress limits are evaluated throughout the temporal and spatial regime to ensure an accurate assessment of the failure potential of a TPBAR.

Burst Stress Allowable

Using experimental data from both uncoated and coated stainless steel 316 tubing, the thick-wall hoop stress at burst for internal pressure loading conditions has been developed for use in the TPBAR LOCA Metric. Both the best-estimate and lower bound polynomial expressions are used to develop the models.

The best estimate and lower bound curves for the thick-wall hoop burst stress were obtained using a seventh order polynomial function given by:

$$\sigma_{burst}(T) = A + B \cdot T + C \cdot T^2 + D \cdot T^3 + E \cdot T^4 + F \cdot T^5 + G \cdot T^6 + H \cdot T^7 \qquad \text{(3d-1)}$$

where σ_{burst} is the thick wall hoop stress at rupture in ksi[2] T is the temperature in °F. The lower bound thick-wall hoop burst curve was selected as the allowable stress limit (BS_{mb}) for evaluation of the primary membrane stress intensity factor of safety. The polynomial function coefficients for the lower bound curve are provided in Table 3d-1. The polynomial expression coefficients are applicable in the temperature range of 500°F to 2000°F. The thick-wall hoop burst stress for temperatures below 500°F use the 500°F value which ensures complete coverage across the range of applicability for the stress analysis.

Table 3d-1: Polynomial Coefficients for the Lower Bound Burst Stress Model[3]

Coefficient	Value
A_{LB}	-1.2182110E+01
B_{LB}	7.4381080E-01
C_{LB}	-1.9142010E-03
D_{LB}	2.5960540E-06
E_{LB}	-2.0691570E-09
F_{LB}	9.4271060E-13
G_{LB}	-2.2702770E-16
H_{LB}	2.2521420E-20

[2] This is a typical unit associated with stress calculations in customary units – 1 ksi is 1000 psi.
[3] These coefficients will yield a thick-wall hoop stress in ksi.

Creep Damage Allowable

A creep damage model was developed from high temperature time-to-failure tests conducted on coated stainless- steel cladding. These tests were performed over a temperature range between 1500°F and 1650°F with rupture times that varied from 50 to 2500 seconds. Using the Larson-Miller model to evaluate the dependency between applied stress, temperature and rupture time, a TPBAR cladding specific C-parameter was derived for use in the creep damage model. The modified Larson-Miller model was then used to construct curves of thick-walled hoop stress as a function of temperature for a constant time to rupture using both best-estimate and lower bound approaches.

The creep rupture damage accumulation model in the TPBAR LOCA metric is composed of five curves that relate the cladding applied stress and temperature to the time required to rupture the cladding. These five curves represent discrete times to failure at 60, 120, 300, 600, and 1200 seconds. The standard form of the polynomial functions is given by the following;

$$\sigma_i = A_i^{tr} + B_i^{tr} \cdot T + C_i^{tr} \cdot T^2 + D_i^{tr} \cdot T^3 + E_i^{tr} \cdot T^4 + F_i^{tr} \cdot T^5 \qquad \text{(3d-2)}$$

where σ_i is the thick-wall hoop stress in ksi, *i* is the time to creep rupture (60, 120, 300, 600, 1200), T is the temperature in °F, and the polynomial function coefficients are provided in Table 3d-2 for the lower bound models.

Table 3d-2: Polynomial Coefficients for the Lower Bound Creep Rupture Model[4]

	Time to Rupture (*seconds*)				
	60	**120**	**300**	**600**	**1200**
$A_{LB}^{t_r}$	-3.00635E+02	7.05494E+02	1.89580E+03	2.56563E+03	2.947790E+03
$B_{LB}^{t_r}$	1.87441E+00	-1.85801E+00	-6.37504E+00	-8.99412E+00	-1.057510E+01
$C_{LB}^{t_r}$	-3.09727E-03	2.37947E-03	9.15790E-03	1.32034E-02	1.577360E-02
$D_{LB}^{t_r}$	2.43353E-06	-1.54278E-06	-6.57487E-06	-9.66391E-06	-1.172150E-05
$E_{LB}^{t_r}$	-9.65345E-10	4.60903E-10	2.30571E-09	3.46904E-09	4.277630E-09
$F_{LB}^{t_r}$	1.54316E-13	-4.76637E-14	-3.14537E-13	-4.87129E-13	-6.116960E-13

The polynomial functions are applicable in the temperature range of 1150°F to 1800°F. To ensure complete coverage across the range of applicability for the stress analysis, the creep rupture stress at temperatures below 1150°F use the 1150°F value. For temperatures above 1800°F, a linear decrease in the creep rupture stress to zero at 1900°F is used to extrapolate these curves above 1800°F.

The polynomial functions are used to calculate the potential for creep rupture using a modified form of the Life Fraction Rule (LFR). The TPBAR LOCA metric tracks the amount of time the applied stress exceeds one or more of these curves.

[4] These coefficients will yield a creep rupture stress in ksi.

$$\Delta t_i^j = t^j - t^{j-1} \; when \; S_{mb}^j \geq \sigma_i^j\left(T^j\right) \tag{3d-3}$$

where *i* represents the discrete creep rupture times, *j* represents the time step number, S_{mb} is the primary membrane plus bending stress intensity and σ_i. When implementing this approach, the application of the above equation is applied only when the stress intensity falls between the creep rupture curves (i.e., the time increment is calculated for the 300 second interval when the primary stress intensity falls between the 120 second and 300 second curves.)

The total time above each of the five creep rupture curves is calculated by:

$$t_i = \sum_{j=1}^{N} \Delta t_i^j \qquad for \; i = 60, 120, 300, 600, 1200 \tag{3d-4}$$

where *N* is the total number of time steps in the LOCA evaluation. To calculate the total accumulated creep damage (or life fraction) for a particular elevation, the time above each creep rupture curve is divided by the time to rupture and these fractions are summed as shown below.

$$D = \; 2 \cdot \left[\frac{t_{60}}{60} + \frac{t_{120}}{120} + \frac{t_{300}}{300} + \frac{t_{600}}{600} + \frac{t_{1200}}{1200}\right] \tag{3d-5}$$

Verification of this approach finds that the modified life fraction rule underestimates the creep damage accumulation as compared to the implementation of the complete life fraction approach that considers the time integration of the entire stress and temperature history. To ensure that this approach remains conservative, a multiplier of two is applied as shown in the above equation.

The accumulated creep damage (D) is then used to assess the potential for failure by the creep rupture mechanism using the following criteria.

D < 1.0 creep rupture not expected
D ≥ 1.0 creep rupture expected

The creep damage allowable limit is applied only to the primary membrane plus bending stress intensities as these stress components are the extended time applied stresses during the event.

The allowable stress limits summarized in this section are applied at each axial division (node) contained within the temperature data provided by the LOCA analysis methodology. The factor of safety from burst rupture and the creep damage factor are evaluated throughout the entire temporal and spatial regime to ensure an accurate assessment of the failure potential of a TPBAR.

SFNB D-RAI 4

Section 4.2.2 of Enclosure 1 of the LAR specifies values for the acceptance criteria that ensure TPBAR structural integrity as listed in Table 4.3.2-1.

(a) Provide the basis or justification for the criterion values listed in Table 4.3.2-1.
(b) Table 4.3.2-1 indicates that criterion values reflect the correction of the error in gamma energy redistribution uncertainty. Please explain how the error in gamma distribution uncertainty is determined and how the corrections are made in the safety factor for offsite power available (OPA) and loss of offsite power (LOOP).

TVA Response to SFNB D-RAI 4(a)

A factor of unity for each of the acceptance criterion indicates that the applied loading has reached the expected loading conditions for component failure. In the case of the primary membrane and bending stress safety factor, a value of unity designates that the stress intensity from the applied loads has reached the lower bound limit for the hoop stress at burst. In the case of the cumulative creep damage ratio, a value of unity signifies that the amount of creep damage accumulated during the applied stress intensity has reached the amount necessary to cause creep rupture.

Using a value of unity for the acceptance criteria will ensure TPBAR structural integrity because of the conservative approach used; 1) to calculate the stress intensities arising from the applied loads and 2) to develop the allowable stress limits with statistical methods to produce lower 95/95 models. A summary of the conservatisms applied within the TPBAR structural integrity methodology is provided in Table 4a-1.

Table 4a-1: TPBAR Structural Integrity Methodology Conservatisms

Description	Conservatism	Impact
Use fuel rod temperatures for TPBAR temperature and internal pressure	Fuel rod temperatures will be higher than a TPBAR by 100 to 200°F[5]	approximately 10% increase in stress intensity approximately 20 to 40% decrease in allowable stress
TPBAR internal void volume	Use minimum internal void volume for pressure calculation	Greater than 5% increase in stress intensity
Cladding tolerance stack up	Worst case fabrication tolerance values used in stress analysis	approximately 2% increase in stress intensity
Cladding corrosion allowance	End of life corrosion thickness on both inner surface and outer surface.	approximately 1% increase in stress intensity

[5] Estimated maximum difference in temperature during the LOCA. The difference between the fuel rod and TPBAR cladding temperatures will decrease at times later in the event.

Table 4a-1: TPBAR Structural Integrity Methodology Conservatisms		
Description	**Conservatism**	**Impact**
Tritium released from the pellet available for gas pressurization	Assume 50 percent of tritium produced is in the pellet available for release	approximately 5% increase the internal gas inventory
Burst criterion	Use lower bound of the burst stress data as allowable limit	approximately 10 to 25% reduction in allowable stress

The conservatisms summarized above maximize the calculated stress intensities and decrease the allowable stress limits such that the figure of merit is reduced for the burst failure (primary membrane and bending stress) and increased for the thermal creep rupture (cumulative creep damage). Thus, the methodology has been developed to provide a bounding estimate of the conditions that could lead to loss of TPBAR structural integrity. By demonstrating that the temperature and stress conditions experienced by a TPBAR during a LOCA event produce a primary membrane plus bending factor of safety greater than unity and a cumulative creep damage ratio less than unity, the likelihood of component failure is sufficiently low to ensure TPBAR survivability.

TVA Response to SFNB D-RAI 4(b)

The treatment for the uncertainty in the gamma energy redistribution is discussed on pages 29-75 and 29-76 of WCAP-16996-P-A, Revision 1, (Reference 1) and the equation for the assumed increase in hot rod and hot assembly relative power is presented on page 29-76 of Reference 1. The power increase in the hot rod and hot assembly due to energy redistribution in the FSLOCA™[6] Evaluation Model (EM) simulations supporting the TPBAR structural integrity analysis was calculated incorrectly. This error resulted in a zero to five percent deficiency in the modeled hot rod and hot assembly rod linear heat rates on a run-specific basis, depending on the as-sampled value for the uncertainty. The effect of the error correction was evaluated against the application of the FSLOCA EM to the WBN Units 1 and 2 TPBAR structural integrity analysis.

The error correction has only a limited impact on the power modeled for a single assembly in the core. Therefore, there is a negligible impact of the error correction on the system thermal-hydraulic response during the postulated LOCA.

Parametric PWR sensitivity studies, derived from a subset of uncertainty analysis simulations covering various design features and fuel arrays, were examined to determine the sensitivity of the analysis results to the error correction. The magnitude of the impact from the error correction was found to be different for the different transient phases (i.e., blowdown versus reflood) based on the PWR sensitivity studies and existing power distribution sensitivity studies. Based on the results from the PWR sensitivity studies, the correction of the error is estimated to

[6] FULL SPECTRUM and FSLOCA are trademarks of Westinghouse Electric Company LLC, its affiliates and/or its subsidiaries in the United States of America and may be registered in other countries throughout the world. All rights reserved. Unauthorized use is strictly prohibited. Other names may be trademarks of their respective owners.

result in a fuel cladding temperature increase of 31°F for the time period relevant to TPBAR structural integrity, which is assumed to also lead to a TPBAR cladding temperature increase of 31°F.

Because the impact was determined based on parametric sensitivity studies and is based on the limiting transient phase, the 31°F temperature increase is applicable to both the LOOP and OPA analyses.

To estimate the effect of changes in the TPBAR cladding temperature on the results of the TPBAR structural integrity analysis, the TPBAR structural integrity calculations were performed with an assumed increase in TPBAR temperature throughout the transient.

The updated TPBAR structural integrity analysis results, including the error correction, were determined using a TPBAR cladding temperature increase of 31°F and are presented in Table 4.3.2-1 of Reference 2.

References

1. WCAP-16996-P-A, Revision 1, “Realistic LOCA Evaluation Methodology Applied to the Full Spectrum of Break Sizes (FULL SPECTRUM LOCA Methodology),” dated November 2016
2. TVA Letter to NRC, CNL-19-051, “Application to Implement the FULL SPECTRUM™[1] LOCA (FSLOCA™[1]) Methodology for Loss-of-Coolant Accident (LOCA) Analysis and New LOCA-specific Tritium Producing Burnable Absorber Rod Stress Analysis Methodology (WBN TS 19-04),” dated January 17, 2020 (ML20017A338)

SFNB D-RAI 5

[[

]]

TVA Response to SFNB D-RAI 5(a)

[

][a,c]

TVA Response to SFNB D-RAI 5(b)

As described in Section 4.2.2 of the LAR, helium is a by-product of the absorption of neutrons by Li-6 and the creation of tritium. The tritium generated is used to compute the helium gas inventory and thereby the initial TPBAR internal gas pressure.

The tritium production **[**

][a,c]

SFNB D-RAI 6

WCAP-18429-P and other documents viewed during the audit, and the LAR indicate that a statistical approach similar to the that used in the FSLOCA Evaluation Model to demonstrate compliance with 10 CFR 50.46 acceptance criteria is used for the LOCA-specific TPBAR stress analysis. Section 4.2.2 of the LAR indicates that a Monte Carlo style uncertainty analysis to construct the FOM related to TPBAR structural integrity is performed. The NRC staff could not identify any documents where the details of either the statistical approach or Monte Carlo style uncertainty analysis for the TPBAR structural integrity analysis were provided.

*Provide details of the statistical approach and/or the Monte Carlo style uncertainty analyses where tolerance limits are constructed for the figures-of-merit related to the TPBAR structural integrity. The response should include sampling size and their origin, type of statistical distribution of samples, **[[ ]]**, analysis methods and other attributes to statistical approach.*

TVA Response to SFNB D-RAI 6

Section 30 of WCAP-16996-P-A, Revision 1, describes the statistical approach utilized in the FSLOCA EM. Analyses performed using the FSLOCA EM follow a Monte Carlo style uncertainty analysis, wherein various contributors to uncertainty are explicitly treated according to their defined uncertainty distributions. Such contributors include model uncertainties and initial/accident condition uncertainties (plant conditions at the time of the postulated LOCA). A sample of postulated LOCAs is numerically simulated, and the figures of merit [peak cladding temperature (PCT), maximum local oxidation (MLO), and core-wide oxidation (CWO)] are computed for each LOCA in the sample. Order statistics are used to create upper tolerance

limits for the population of possible LOCAs for the figures of merit. A 95% confidence statement is made that 95% of all postulated LOCAs will result in PCT, MLO, and CWO less limiting than the derived upper tolerance limits. Those tolerance limits are then compared against the acceptance criteria to confirm compliance with 10 CFR 50.46.

The statistical statements of probability and compliance refer to the population of results as predicted by the numerical simulation tool, the analysis approach, and the uncertainty distributions of the various uncertainty contributors; any conservatism in those areas serves only to increase the probability/confidence for the real system, albeit by an unquantified amount.

A similar approach to the typical 10 CFR 50.46 analysis is followed for the TPBAR structural integrity analysis, in that a numerical surrogate for the physical system is constructed, and then a statistical analysis is performed to construct tolerance limits for the figures of merit related to the TPBAR structural integrity: (1) rupture due to primary membrane and bending stresses, and (2) rupture due to creep damage. The derived tolerance limits are compared to acceptance criteria (failure thresholds) to confirm compliance (structural integrity).

A typical FSLOCA EM Region II (LBLOCA) analysis consists of WCT-TF2 simulations **[**

][a,c]

In analyses performed using the FSLOCA EM, **[**

][a,c]

The goal of the TPBAR structural integrity analysis is to demonstrate that TPBARs maintain structural integrity (i.e., survive) during a LBLOCA such that their presence can be credited in post-LOCA criticality calculations. **[**

][a,c]

In the TPBAR structural integrity analysis, a sample of postulated LOCAs is simulated in WCT-TF2 to determine the resulting fuel rod cladding temperatures. The TPBAR cladding

temperature is assumed to equal the fuel rod cladding temperature **[**
][a,c] The TPBAR cladding temperature is then used to calculate margins to failure thresholds. **[**
][a,c]

The FSLOCA EM statistical process as described in Section 30 of WCAP-16996-P-A, Revision 1 **[**

][a,c]

[

][a,c]

The FSLOCA EM is designed to provide realistic, yet conservative, predictions for peak cladding temperature and time-at-temperature (oxidation). Therefore, the models, uncertainty ranges, initial and boundary conditions, and plant operational assumptions are all designed to account for the appropriate phenomena and to conduct the analysis in a manner that provides realistic, yet conservative, PCT and MLO predictions. Because the nuclear fuel cladding temperature is used directly from the WCT-TF2 simulations as a basis for the TPBAR cladding temperatures in the TPBAR structural integrity analysis, it can be stated that the modeled TPBAR cladding temperatures are conservative. Additional conservatism with respect to the TPBAR cladding temperature in comparison to the nuclear fuel cladding temperature is associated with the assumption that the TPBAR cladding temperature follows the nuclear fuel cladding temperature exactly. Beyond these conservatisms, the primary membrane and bending stress and creep rupture damage stress are treated using a deterministic method and contain bounding estimates for geometric parameters, ensuring additional conservatism in the calculated tolerance limits. Some conservative aspects of the stress intensity calculations are listed in Table 4.2.2-1 in Enclosure 1 of the LAR.

Limitation and Condition (L&C) number 11 in the NRC Safety Evaluation Report (SER) of the FSLOCA EM (WCAP-16996-P-A, Revision 1) is applicable to the TPBAR structural integrity analysis, with the relevant portion as follows for Region II (LBLOCA) analyses:

> The **[** **]**[a,c], seed, analysis inputs, and **[**
> **]**[a,c] will be declared and documented prior to performing the uncertainty analyses. The **[**
> **]**[a,c] will not be adjusted as a result of the outcome.

This L&C is adapted and applied to TPBAR structural integrity analyses as follows. The Region II (LBLOCA) simulations performed as part of the TPBAR structural integrity analysis therefore follow the intent of this L&C.

> The **[** **]**[a,c], seed, analysis inputs for the WCOBRA/TRAC-TF2 simulations supporting the TPBAR structural integrity analysis, and **[** **]**[a,c] will be declared and documented prior to performing the uncertainty analyses. The **[** **]**[a,c] will not be adjusted as a result of the outcome.

L&C number 15 in the NRC SER is also applicable to the TPBAR structural integrity analysis and requires that the Region II analysis be executed twice; once assuming loss-of-offsite power (LOOP) and once assuming offsite power available (OPA). The results from both analysis executions should be shown to be in compliance with the LOCA limits. Similarly, the TPBAR structural integrity analysis is performed for both OPA and LOOP configurations, to ensure that the results for both configurations are within the TPBAR structural integrity analysis limits.

Additionally, L&C number 15 requires that the **[**

][a,c] L&C number 15 is therefore adapted for the TPBAR structural integrity analysis as follows:

> The **[**
> **]**[a,c]

For the WBN Units 6-1 and 2 TPBAR structural integrity analysis, **[**

][a,c]

The LOCA transient response for the previously determined and documented cases (LOCA scenarios) in the sample for each offsite power condition (LOOP and OPA) is calculated. The TPBAR structural integrity results from the full sample for each of the offsite power conditions (LOOP and OPA) are processed and compared against the acceptance criteria.

As described in Section 4.3.2 of the LAR, “Enclosure 3 describes an analysis performed for WBN Units 1 and 2, using the FSLOCA Evaluation Model to satisfy the 10 CFR 50.46 acceptance criteria. For the separate TPBAR structural integrity analysis, the same WCT-TF2 input model was used. Also, the same major plant parameter and analysis assumptions (i.e., Tables 1 through 3 in Enclosure 3) were used.”

Table 6-1 [

]a,c

[	
	]a,c

Table 6-2 [ ]a,c

[	
	]a,c

[

]a,c

SNSB D-RAI 1

In Enclosures 3 and 4 to the LAR, in response to Limitation and Condition 12, TVA states that a bounding plant-specific dynamic pressure loss from the steam generator secondary-side to the main steam safety valves was modeled in the Watts Bar Units 1 and 2 analysis. Provide the value used for the bounding plant-specific analysis and a brief explanation for why it is a way to adequately account for the pressure loss.

TVA Response to SNSB D-RAI 1

Limitation and Condition (L&C) 12 states: "In plant-specific applications of the FSLOCA™ EM, a check will be performed to confirm that effects associated with dynamic pressure losses from the steam generator secondary side to the main steam safety valves (MSSVs) are properly considered and adequately accounted for in the plant model used for the design-basis LOCA analyses consistent with NRC Information Notice 97-09, 'Inadequate Main Steam Safety Valve (MSSV) Set Points and Performance Issues Associated with Long MSSV Inlet Piping.' SBLOCA performance is dependent on secondary pressure as it establishes primary pressure, and the consequential emergency core cooling system injection rate and potential for and degree of core uncovery."

As discussed in the response to Request for Additional Information (RAI) 132 as contained in LTR-NRC-14-4 (Reference 1) and the Appendices to WCAP-16996-P-A, Revision 1 (Reference 2), **[**

][a,c]

To comply with the L&C in the WBN Units 1 and 2 analysis and ensure that the pressure losses have been accounted for, the initial opening pressure of the first stage MSSV was modeled as 10 psi higher than the plant-specific first stage MSSV set pressure, plus uncertainty (1246 psia). The pressure loss in the line between the steam generator and the MSSV at full rated first stage flow is 20 psi. At the beginning of the natural circulation period of the limiting transient from the Region I uncertainty analysis, the flow through each MSSV is approximately 25% of the rated flow, and diminishes after that, which would lead to a pressure loss of approximately 1.25 psi (20 psi x $.25^2$ = 1.25 psi) or less. As such, the 10 psi additional modeled pressure is more than adequate to account for the pressure loss.

References

1. Westinghouse letter to NRC, LTR-NRC-14-4, "Submittal of Westinghouse Responses to 'WCAP-16996-P, 'Realistic LOCA Evaluation Methodology Applied to the Full Spectrum of Break Sizes (FULL SPECTRUM LOCA Methodology)' Request for Additional Information - Set 8 RAIs 127, 132-135 and 137-139' (Proprietary/Non-Proprietary), Project 700, TAC No. ME5244," dated January 30, 2014 (ML14041A162)
2. WCAP-16996-P-A, Revision 1, "Realistic LOCA Evaluation Methodology Applied to the Full Spectrum of Break Sizes (FULL SPECTRUM LOCA Methodology)," dated November 2016

SNSB D-RAI 2

In Enclosures 3 and 4 to the LAR, TVA states that inboard grid deformation due to combined LOCA and seismic loads is not calculated to occur for Watts Bar Units 1 and 2. Discuss how TVA came to this determination.

TVA Response to SNSB D-RAI 2

The FSLOCA EM analysis does not affect the existing analysis of record related to combined LOCA and seismic loads, and this conclusion is retained from prior calculations and is credited in the current LOCA design basis analyses. As described in Section 4.2.1.3.5 of the WBN dual-unit Updated Final Safety Analysis Report (UFSAR) regarding the combined LOCA and seismic loads,

> "Only a small (outer) portion of the core experienced significant grid impact forces. The maximum grid impact forces are required to be less than the allowable grid crush strength. A calculation of the maximum LOCA and seismic grid impact forces, combined using the square root sum of the squares method (in accordance with NUREG 0800, Section 4.2, Appendix A), demonstrated that the maximum value is less than the allowable grid strength for both the homogeneous core (RFA-2 with IFMs) and the mixed core (RFA-2 with IFMs and V+/P+ without IFMs)."

Enclosure 3

Westinghouse Electric Company LLC Application for Withholding Proprietary Information From Public Disclosure (Affidavit CAW-20-5080)

AFFIDAVIT

COMMONWEALTH OF PENNSYLVANIA:
COUNTY OF BUTLER:

(1) I, Korey L. Hosack, have been specifically delegated and authorized to apply for withholding and execute this Affidavit on behalf of Westinghouse Electric Company LLC (Westinghouse).

(2) I am requesting the proprietary portions of WAT-D-12626 Revision 1 P-Attachment and TTP-20-105 be withheld from public disclosure under 10 CFR 2.390.

(3) I have personal knowledge of the criteria and procedures utilized by Westinghouse in designating information as a trade secret, privileged, or as confidential commercial or financial information.

(4) Pursuant to 10 CFR 2.390, the following is furnished for consideration by the Commission in determining whether the information sought to be withheld from public disclosure should be withheld.

(i) The information sought to be withheld from public disclosure is owned and has been held in confidence by Westinghouse and is not customarily disclosed to the public.

(ii) Public disclosure of this proprietary information is likely to cause substantial harm to the competitive position of Westinghouse because it would enhance the ability of competitors to provide similar technical evaluation justifications and licensing defense services for commercial power reactors without commensurate expenses. Also, public disclosure of the information would enable others to use the information to meet NRC requirements for licensing documentation without purchasing the right to use the information.

AFFIDAVIT

(5) Westinghouse has policies in place to identify proprietary information. Under that system, information is held in confidence if it falls in one or more of several types, the release of which might result in the loss of an existing or potential competitive advantage, as follows:

(a) The information reveals the distinguishing aspects of a process (or component, structure, tool, method, etc.) where prevention of its use by any of Westinghouse's competitors without license from Westinghouse constitutes a competitive economic advantage over other companies.

(b) It consists of supporting data, including test data, relative to a process (or component, structure, tool, method, etc.), the application of which data secures a competitive economic advantage (e.g., by optimization or improved marketability).

(c) Its use by a competitor would reduce his expenditure of resources or improve his competitive position in the design, manufacture, shipment, installation, assurance of quality, or licensing a similar product.

(d) It reveals cost or price information, production capacities, budget levels, or commercial strategies of Westinghouse, its customers or suppliers.

(e) It reveals aspects of past, present, or future Westinghouse or customer funded development plans and programs of potential commercial value to Westinghouse.

(f) It contains patentable ideas, for which patent protection may be desirable.

(6) The attached documents are bracketed and marked to indicate the bases for withholding. The justification for withholding is indicated in both versions by means of lower-case letters (a) through (f) located as a superscript immediately following the brackets enclosing each item of information being identified as proprietary or in the margin opposite such information. These

AFFIDAVIT

lower-case letters refer to the types of information Westinghouse customarily holds in confidence identified in Sections (5)(a) through (f) of this Affidavit.

I declare that the averments of fact set forth in this Affidavit are true and correct to the best of my knowledge, information, and belief.

I declare under penalty of perjury that the foregoing is true and correct.

Executed on: 2020 08 13

Korey L. Hosack, Manager
Licensing, Analysis, & Testing